

Growing “Nanofruit” Textures on Photo-Crosslinked SU-8 Surfaces through Layer-by-Layer Grafting of Hyperbranched Poly(Ethyleneimine)

Jamie Ford,[†] Seth R. Marder,[‡] and Shu Yang^{*,†}

Department of Materials Science and Engineering, University of Pennsylvania, 3231 Walnut Street, Philadelphia, Pennsylvania 19104, and School of Chemistry & Biochemistry and Center for Organic Photonics and Electronics, Georgia Institute of Technology, 901 Atlantic Drive Northwest, Atlanta, Georgia 30332-0400

Received July 13, 2008. Revised Manuscript Received December 3, 2008

We report the growth of hierarchical nanostructures on a photo-crosslinked SU-8 surface through alternating layer-by-layer Michael addition reactions between poly(ethyleneimine) (PEI) and dipentaerythritol pentaacrylate (SR399) to generate grafted hyperbranched poly(ester amines) (HPEA). Initial surface treatment with acryloyl chloride (AC) in toluene partially swelled the polymer network, resulting in the formation of “nano-cranberry” domes (~100 nm in diameter), whose size and density could be varied by the choice of solvent, concentration, and reaction time of acryloyl chloride. The subsequent layer-by-layer grafting of hyperbranched PEI led to the formation of surfaces evocative of “nano-strawberries”, “nano-raspberries” and “nano-pineapples”, each of which consisted of ~16–21 nm “nanoseeds” grown on top of and between the nanodomains. The complexity and coverage of the seeds can be manipulated by the generation and molecular weight of PEI grafts. In contrast, when the cross-linked SU-8 surface was initially treated with (aminopropyl)triethoxy silane (APTES), a smooth surface with uniform coverage of nanomotifs (19.4 ± 5.6 nm) was obtained, independent of the PEI generation. Because the hierarchical hyperbranched poly(ester amines) “nanofruits” are grown from a photopatterned substrate, it will allow us to harness the underlying micropatterns for various applications, including surface wetting, adhesion, and biomimetic mineralization.

Introduction

Bio-organisms often exhibit an exquisite array of hierarchical organization with multiscale structures as exemplified by the iridescence in blue *Morpho rhetenor* butterflies,¹ the waveguiding properties in diatom exoskeletons,² the self-cleaning ability of lotus leaves,³ and the dry adhesion of Gecko foot hairs.⁴ These examples provide inspiration for the development of new functional hybrid materials. To mimic hierarchical organization in Nature, one of the emerging strategies is the convergence of top-down micro-fabrication and bottom-up nanoassembly, using lithographically patterned polymer microstructures as predefined templates to graft polymer brushes with desired functionality to fine-tune the nanoscale motifs.

SU-8 is a bisphenol A novolac resin derivative with an average of eight epoxy groups. Because of its high thermal and mechanical strength ($T_g > 200$ °C, and Young’s modulus of up to 5 GPa), it has been widely used as a thick negative-tone resist to fabricate microelectromechanical systems

(MEMS) devices,⁵ microfluidic channels,⁶ high-aspect ratio microstructures, 3D photonic structures,⁷ and substrates for biological applications.^{8,9} However, the crosslinked SU-8 surface is relatively inert and surface modification is necessary to introduce functional groups and improve their surface coverage. Through chemical reaction,¹⁰ hot wire chemical vapor deposition of ammonia,¹¹ physical grafting and metal deposition,¹⁰ amino groups, polyethylene oxide (PEO) chains, and metal thin films have been incorporated on the patterned SU-8 surfaces either homogeneously or selectively. However, the population of functional groups introduced on the SU-8 surface is rather small. For example, physical grafting of PEO to an SU-8 surface leads to a density of ~1 PEO chain per 15×15 nm² or less.¹⁰ The low density of functional groups makes it difficult to direct further reactions, such as sol–gel reactions or grafting DNA molecules to the surface.

* Corresponding author. E-mail: shuyang@seas.upenn.edu.

[†] University of Pennsylvania.

[‡] Georgia Institute of Technology.

(1) Vukusic, P.; Sambles, J. R. *Nature* **2003**, *424*, 852.

(2) Fuhrmann, T.; Landwehr, S.; El Rharbi-Kucki, M.; Sumper, M. *Appl. Phys. B: Lasers Opt.* **2004**, *78*, 257.

(3) Barthlott, W.; Neinhuis, C. *Planta* **1997**, *202*, 1.

(4) Autumn, K.; Liang, Y. A.; Hsieh, S. T.; Zesch, W.; Chan, W. P.; Kenny, T. W.; Fearing, R.; Full, R. J. *Nature* **2000**, *405*, 681.

(5) Lorenz, H.; Despont, M.; Fahrni, N.; LaBianca, N.; Renaud, P.; Vettiger, P. *J. Micromech. Microeng.* **1997**, *7*, 121.

(6) Ribeiro, J. C.; Minas, G.; Turmezei, P.; Wolfenbutter, R. F.; Correia, J. H. *Sens. Actuators, A* **2005**, *123–24*, 77.

(7) Moon, J. H.; Ford, J.; Yang, S. *Polym. Adv. Technol.* **2006**, *17*, 83.

(8) Wang, Y. L.; Pai, J. H.; Lai, H. H.; Sims, C. E.; Bachman, M.; Li, G. P.; Allbritton, N. L. *J. Micromech. Microeng.* **2007**, *17*, 1371.

(9) Kastantin, M. J.; Li, S.; Gadre, A. P.; Wu, L. Q.; Bentley, W. E.; Payne, G. F.; Rubloff, G. W.; Ghodssi, R. *Sens. Mater.* **2003**, *15*, 295.

(10) Moon, J. H.; Kim, A. J.; Crocker, J. C.; Yang, S. *Adv. Mater.* **2007**, *19*, 2508.

(11) Joshi, M.; Kale, N.; Lal, R.; Rao, V. R.; Mukherji, S. *Biosens. Bioelectron.* **2007**, *22*, 2429.

One common strategy to amplify the surface coverage of functional groups is to graft hyperbranched or dendritic polymer brushes. Because of their unique architectures and high concentration of surface terminal groups,¹² hyperbranched and dendritic polymers are of interest in a wide range of applications, including metal complexation,¹³ sensors,¹⁴ adhesion,¹⁵ energy conversion and storage,¹⁶ and drug delivery.¹⁷ Of particular interest in this letter are polyamine brushes, which have been shown to be templates for the directed deposition of inorganic nanoparticles.^{18–22} Through Michael addition and amidation reactions between small molecule building blocks, such as ethylenediamine (EDA) and methyl acrylate (MA) or multifunctional acrylates,^{12,23–29} dendrons and hyperbranched poly(ester amines) have been grafted on various solid substrates, including glass, mica, polystyrene, and carbon nanotubes.³⁰ The chemical nature, number of surface functional groups, and the hydrodynamic radius of polymers³¹ can be fine-tuned with reaction generation. Recently, Weatherspoon et al. reported a strategy to amplify the density of hydroxyl groups on the surface of an aminosilane diatom frustule through alternating reactions between tris(2-aminoethyl)amine and dipentaerythritol pentaacrylate (SR399), leading to a continuous thin coating of SnO₂ on the diatom frustule surface.³²

Here, we adapted that surface amplification strategy to graft hyperbranched poly(ester amines) (HPEA) through alternating reactions between poly(ethyleneimine) (PEI) and SR399 on photo-crosslinked SU-8, and studied the hierarchical organization and evolution of HPEA as a function of generation number. By employing a polyamine chain, as opposed to small molecules, we can quickly build up a large number of surface functional groups and concomitantly vary the surface morphology by fine-tuning the molecular weight and architecture of the polymer brushes. Interestingly, we

found that the surface morphology was critically dependent on the initial surface modification chemistry and the choice of solvent. When the photo-crosslinked SU-8 surface was treated with acryloyl chloride (AC) in marginally good solvents of SU-8, including anisole, toluene, and xylene, "nano-cranberry" domes (~100 nm in diameter) appeared, and the dome density could be varied by the concentration and reaction time. The nanocranberry formation can be attributed to a synergistic effect of solvent-surface interactions and the reaction between AC and SU-8. As the HPEA generation increased, the texture of the surfaces of the "nano-cranberry" domes evolved into those evocative of "nano-strawberries", "nano-raspberries", and "nano-pineapples", consisting of ~16–21 nm seedlike nanomotifs grown on top of and between the nanocranberries. The complexity and coverage of the "nanoseeds" are dependent on the generation of HPEA and the molecular weight of PEI. In contrast, when the crosslinked SU-8 surface was treated with (aminopropyl)triethoxy silane (APTES), a smooth surface uniformly covered by nanostructures (~20 nm) was obtained. Further layer-by-layer PEI/SR399 grafting did not reveal any dual-level nanostructures on the SU-8 surface. We believe the study of polymer brush morphology and its evolution on photopatterned substrates will broaden the range of design strategies to synthesize novel nanomaterials by harnessing the underlying micropatterns, providing a basis to manipulate macroscopic material properties.

Experimental Section

Unless noted, all chemicals were purchased from Aldrich and used as received.

SU-8 Film Preparation. SU-8 2 (MicroChem Corp.) was spin-cast on Si wafers at 3000 RPM for 30 s. The films were prebaked at 65 °C for 60 s and soft-baked at 95 °C for 60 s. The films were exposed to UV light (B-100AP, Blak-Ray) through a photomask with 180 μm line patterns²² at an intensity of 7 mW/cm² for 120 s, followed by a two-step post-exposure bake at 65 °C for 60 s and 95 °C for 60 s, respectively. The films were developed in propylene glycol methyl ether acetate (PGMEA) and rinsed with isopropyl alcohol.

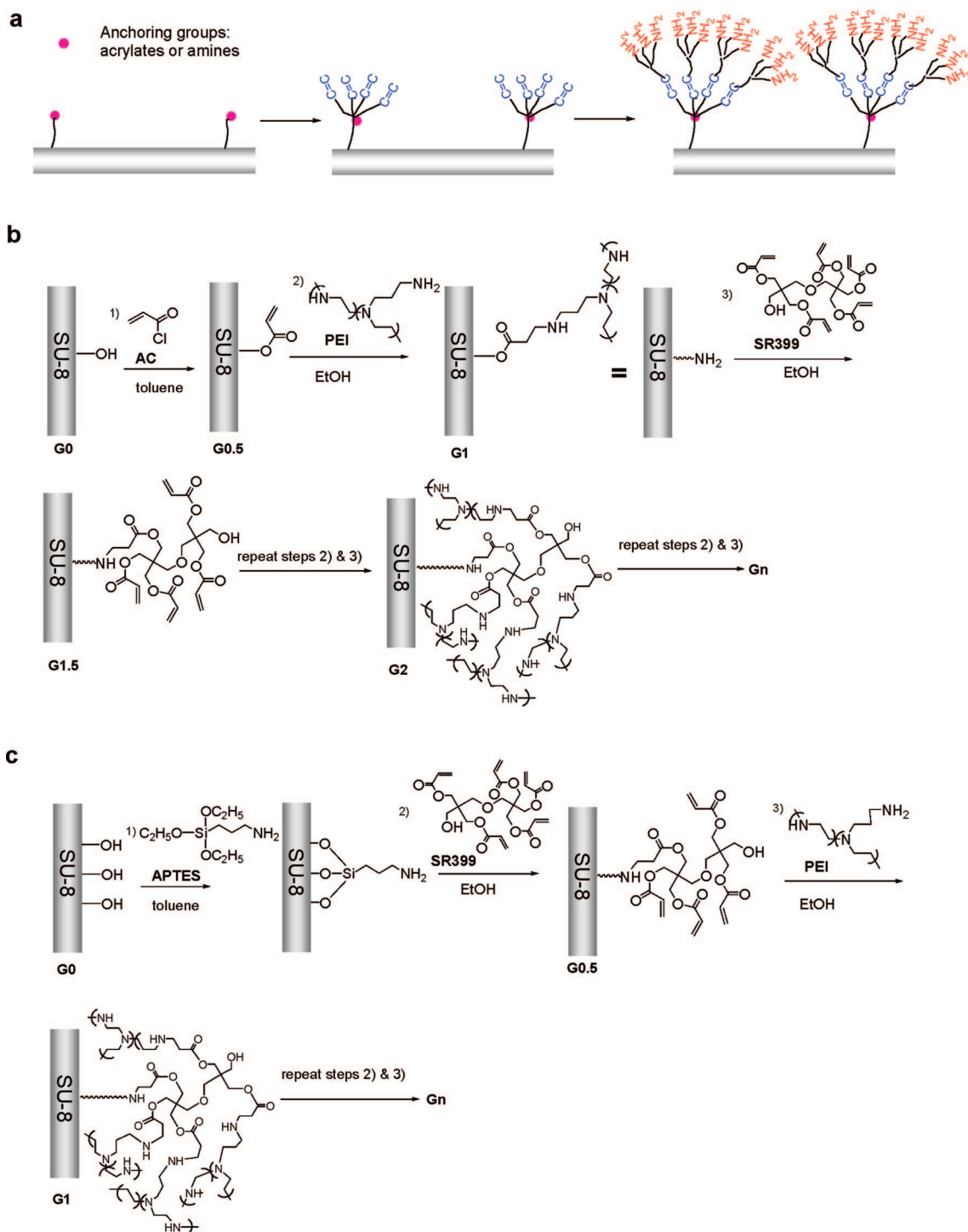
Surface Acrylation. Patterned SU-8 films were soaked in a solution of 100 mM acryloyl chloride (AC) (81.2 μL) dissolved in 9.919 mL of toluene for 5–120 min. The films were then washed three times with fresh toluene and rinsed with isopropyl alcohol.

Surface Amination by APTES. Patterned SU-8 films were soaked in a toluene solution of 3-aminopropyl triethoxysilane (APTES) (213 mM, 5 vol%) for 60 min, followed by washing with copious toluene and isopropyl alcohol.

Grafting of Hyperbranched Polyamines. Polyamines were introduced onto acrylated surfaces by soaking the film for 60 min in a 1.0 mg/mL PEI/ethanol solution. Acrylates were introduced onto amine surfaces by soaking the film in a 20% (v/v) SR399 (Sartomer)/ethanol solution for 60 min. The films were washed three times with copious ethanol before exposure to PEI in the next step. PEI of various molecular weights were used, including MW = 600 (branched, Aldrich), 1800 (branched, Polysciences, Inc.), 2500 (linear, Polysciences, Inc.), and 10 000 g/mol (branched, Polysciences, Inc.). Branched PEI has a primary: secondary: tertiary amine ratio of 1:2:1 with a general backbone of (CH₂CH₂NH)_x and randomly distributed branching sites. Linear PEI contains only secondary amines in the backbone and the chains are terminated with primary amines.

- (12) Tomalia, D. A.; Naylor, A. M.; Goddard, W. A., III *Angew. Chem., Int. Ed.* **1990**, *29*, 138.
- (13) Tran, M. L.; Gahan, L. R.; Gentle, I. R. *J. Phys. Chem. B* **2004**, *108*, 20130.
- (14) Wells, M.; Crooks, R. M. *J. Am. Chem. Soc.* **1996**, *118*, 3988.
- (15) Tully, D. C.; Frechet, J. M. *J. Chem. Commun.* **2001**, *2001*, 1229.
- (16) Tsubokawa, N.; Kotama, K.; Saito, H.; Nishikubo, T. *Comp. Interf.* **2003**, *10*, 609.
- (17) Stiriba, S.-E.; Frey, H.; Haag, R. *Angew. Chem., Int. Ed.* **2002**, *41*, 1329.
- (18) Patwardhan, S. V.; Clarson, S. J. *Polym. Bull.* **2002**, *48*, 367.
- (19) Knecht, M. R.; Wright, D. W. *Langmuir* **2004**, *20*, 4728.
- (20) Jin, R.-H.; Yuan, J.-J. *Macromol. Chem. Phys.* **2005**, *206*, 2160.
- (21) Xu, M.; Gratson, G. M.; Duoss, E. B.; Shepherd, R. F.; Lewis, J. A. *Soft Matter* **2006**, *2*, 205.
- (22) Ford, J.; Yang, S. *Chem. Mater.* **2007**, *19*, 5570.
- (23) Pollock, N.; Fowler, G.; Twyman, L. J.; McArthur, S. L. *Chem. Comm.* **2007**, *2007*, 2482.
- (24) Kaneko, Y.; Imai, Y.; Shirai, K.; Yamauchi, T.; Tsubokawa, N. *Colloids Surf., A* **2006**, *289*, 212.
- (25) Tsubokawa, N.; Ichioka, H.; Satoh, T.; Hayashi, S.; Fujiki, K. *React. Funct. Polym.* **1998**, *37*, 75.
- (26) Tsubokawa, N.; Satoh, T.; Murota, M.; Sato, S.; Shimizu, H. *Polym. Adv. Technol.* **2001**, *12*, 596.
- (27) Zhang, L.; Bo, Z.; Zhao, B.; Wu, Y.; Zhang, X.; Shen, J. *Thin Solid Films* **1998**, *327–329*, 221.
- (28) Tang, L.; You, H.; Wu, J.; Yu, K.; Tang, X. *Colloids Surf., A* **2006**, *275*, 177.
- (29) Tang, L.; You, H.; Feng, J. *Thin Solid Films* **2007**, *515*, 2998.
- (30) Kehat, T.; Goren, K.; Portnoy, M. *New J. Chem.* **2007**, *31*, 1218.
- (31) Tomalia, D. A. *Prog. Polym. Sci.* **2005**, *30*, 294.
- (32) Weatherspoon, M. R.; Dickerson, M. B.; Wang, G.; Cai, Y.; Shian, S.; Jones, S. C.; Marder, S. R.; Sandhage, K. H. *Angew. Chem., Int. Ed.* **2007**, *46*, 5724.

Scheme 1. Illustration of the Construction of Hyperbranched Poly(Ester Amine) Chains Layer-by-Layer on Photo-Crosslinked SU-8 Surfaces^a



^a (a) Schematics of the hyperbranched poly(ester amine) growth. The photo-crosslinked SU-8 surface is treated with (b) acryloyl chloride in toluene to introduce initial acrylate groups, or (c) APTES in toluene to introduce amino groups. After the initial surface modification, dipentaerythritol pentaacrylate (SR399) and PEI are grafted to the surface through alternating Michael addition reactions.

Characterization. FT-IR spectra were collected at resolution of 1.93 cm^{-1} on a Nicolet 450 FT-IR equipped with an MCT/B detector. Tapping-mode atomic force microscopy (AFM) was performed on Digital Instruments Nanoscope IIIa (Santa Barbara, CA) with antimony-doped silicon tapping-mode cantilevers with resonant frequencies between 290 and 327 kHz and tip radii between 8 and 10 nm. Images were captured at 512×512 lines at 1.0 Hz and analyzed with Digital Instruments software. Scanning electron microscopy (SEM) images were obtained with a FEI Strata

DB235 Focused Ion Beam (FIB) at voltage of 5 KeV and with a JEOL 7500F HRSEM at 2 KeV.

Results and Discussion

Polyamines, including poly(phenylene vinylene), poly(allylamine), poly(L-arginine), poly(L-lysine), and PEI, are of interest as structural templates to direct the synthesis of inorganic nanoparticles with a wide variety of morphologies,^{18–22} mim-

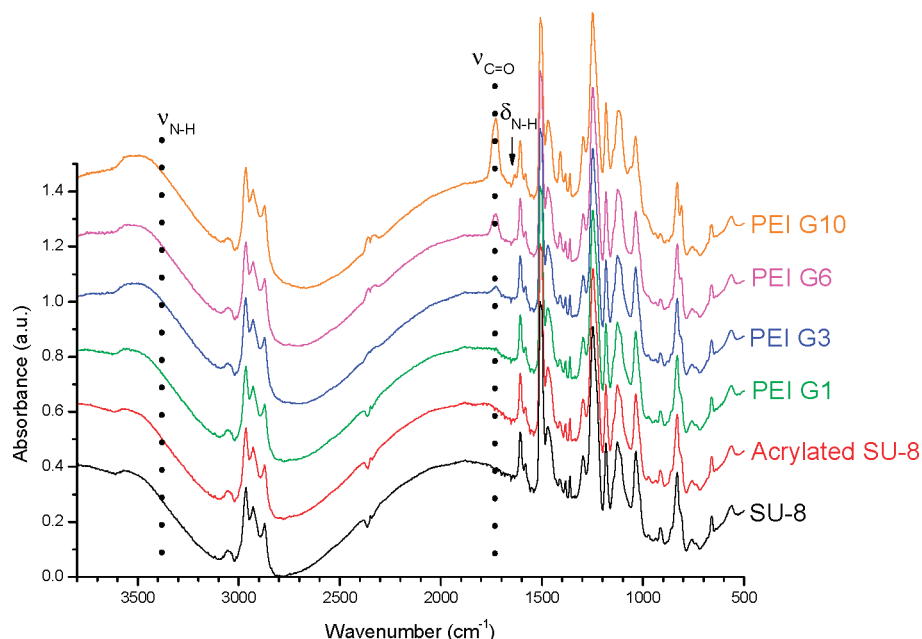


Figure 1. FT-IR spectra of SU-8 films treated with 100 mM acryloyl chloride/toluene solution, followed by grafting with PEI (MW = 10 000 g/mol) at different generations. Increased absorbance at 3380 and 1728 cm^{-1} are indicative of the tethering of PEI and acrylates on surface, respectively. The arrow indicates the appearance of a new peak, corresponding to N–H bending vibration (amide II band).³⁴

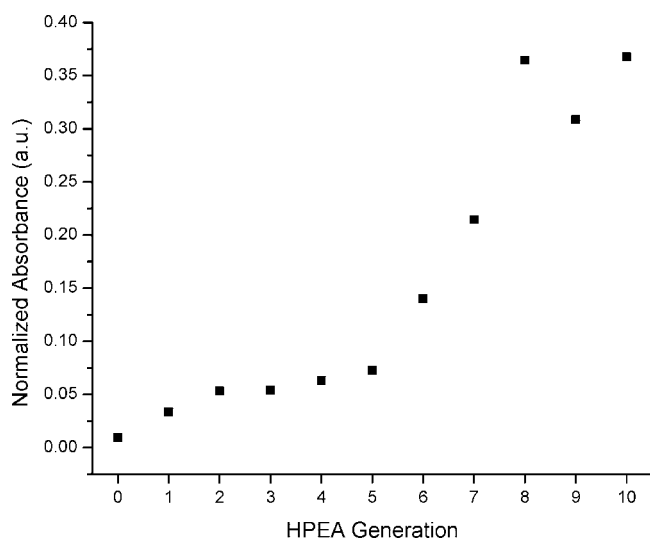


Figure 2. Normalized FT-IR absorbance at 1728 cm^{-1} of SU-8 films as a function of generation of grafted HPEA. The SU-8 films were initially treated with 100 mM acryloyl chloride/toluene solution for 120 min.

icking biomineralization templated by specialized proteins or polypeptides.³³ To graft polyamines onto a highly crosslinked and rather inert patterned SU-8 surface, it is essential to modify the surface by introducing grafting sites. Here, we investigate two strategies to functionalize the SU-8 surface with acrylates or amino groups, followed by layer-by-layer Michael addition reactions to build up HPEA on the surface (Scheme 1). As illustrated in Scheme 1b, the patterned SU-8 templates are treated with acryloyl chloride (AC) in toluene to introduce an initial acrylate on the surface (G0.5). PEI then reacts with the acrylated SU-8, forming C–N bonds between acrylates and amines through a Michael addition reaction, resulting in the polyamine-terminated surface (G1).

Alternatively, if the SU-8 surface is exposed directly to an aminosilane, such as APTES, amino groups can be introduced directly on the surface. When the amine-terminated surface is exposed to the multifunctional acrylate, SR399, an acrylate-terminated surface is generated, which can be exposed to PEI to generate a polyamine-terminated surface (G2). Through this layer-by-layer grafting process, a large number of amine or acrylate groups on the SU-8 surface is quickly built up and amplified. This process can be repeated as many times as desired.

To confirm the grafting of SR399 and PEI, we collected the FT-IR spectra of the SU-8 films at each grafting step. On the surface treated with AC, followed by alternating PEI/SR399 reactions, there is an increase in intensity at 3380 cm^{-1} (N–H stretch of the secondary amine), and appearance of a new peak at 1728 cm^{-1} (C=O stretch, ester amine), whose intensity increases as a function of grafting generation (Figure 1). To quantify the surface coverage of amine and amine-ester groups on SU-8, we normalized the absorbance at 1728 cm^{-1} using the peak at 1506 cm^{-1} (C=C stretch, aromatic ring) from the SU-8 backbone as the internal reference. A moderate but steady increase of absorbance at 1728 cm^{-1} was observed for the first five generations (see Figure 2), followed by a sharp increase afterward. The initial slow growth of HPEA can be attributed to the limited number of available amine and acrylate groups on surface, followed by more rapid growth in a dendritic manner. We note that after the sixth-generation PEI layer was grafted, a new shoulder at 1645 cm^{-1} [N–H bending vibration (amide II band)]³⁴ appeared (Figure 1), further confirming a high density of amines present on the surface.

Phase AFM images of the hyperbranched poly(ester amine) grafted on SU-8 surface show fascinating hierarchical

(33) Meldrum, F. C. *Int. Mater. Rev.* **2003**, *48*, 187.

(34) Silverstein, R. M.; Webster, F. X. *Spectrometric Identification of Organic Compounds*, 6th ed.; John Wiley & Sons: New York, 1998.

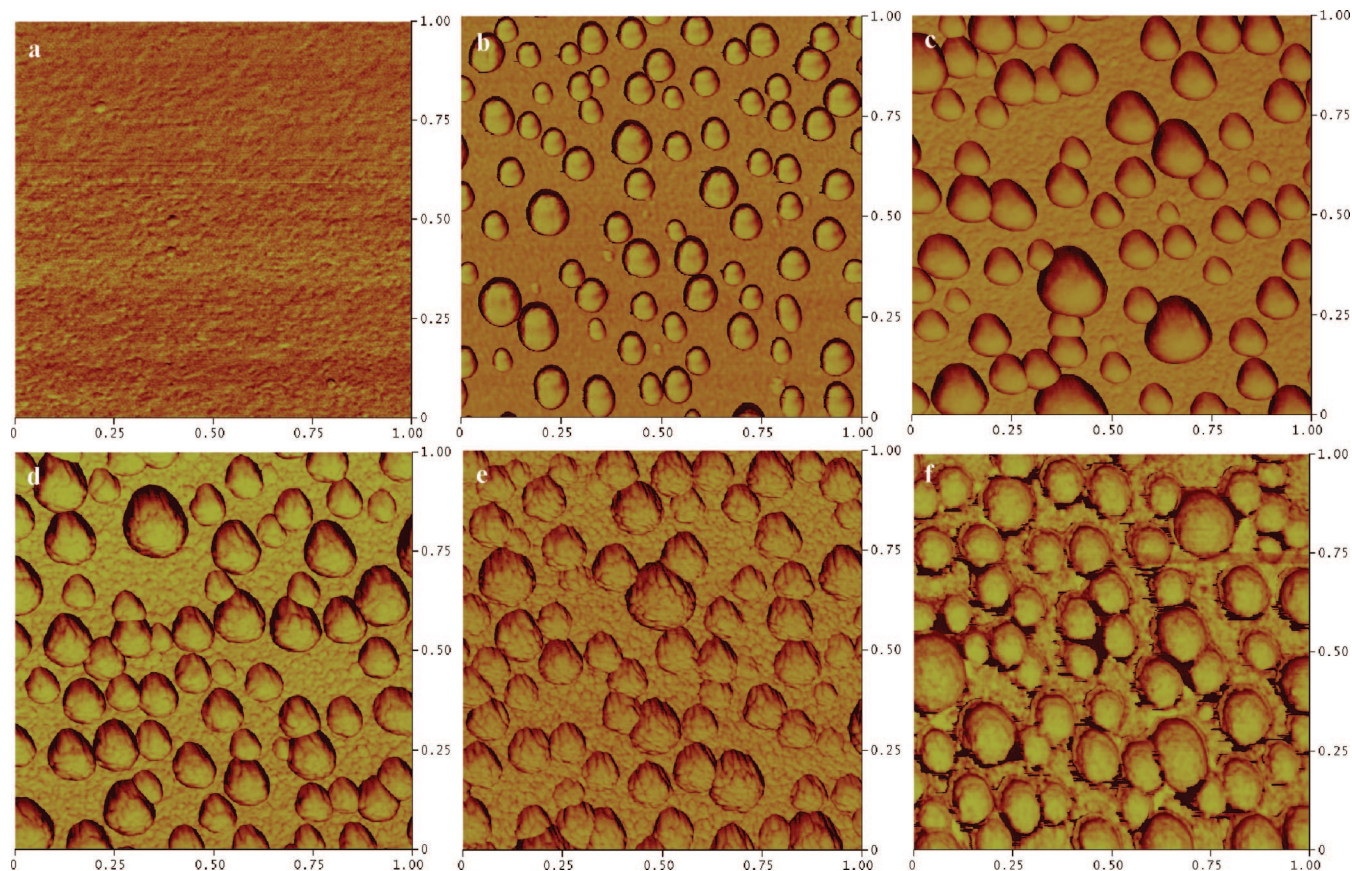


Figure 3. Phase AFM images of SU-8 surface at different surface functionalization stages, showing the gradual growth of textures evocative of various “nanofruits” over branching generations. (a) Bare SU-8 after photocrosslinking. (b) “Nano-cranberries” on SU-8 surface when treated with 100 mM acryloyl chloride/toluene for 120 min, followed by grafting PEI (MW = 10 000 g/mol) at different generations (c–f). (c) G1, (d) G3, “nano-strawberries”, (e) G6, “nano-raspberries”, and (f) G10, “nano-pineapples”. Scale = $1 \mu\text{m} \times 1 \mu\text{m}$.

morphologies that transition from hemispherical “nano-cranberries” to “nano-strawberries”, “nano-raspberries”, and “nano-pineapples” as the generation of PEI grafts increases (Figure 3). Although the untreated SU-8 surface was very smooth ($R_q = 0.392 \text{ nm}$) (Figure 3a), hemispherical “nano-cranberries” appeared after the surface was treated with 100 mM AC/toluene solution for 120 min (Figure 3b). The domes were $82 \pm 16 \text{ nm}$ in diameter and 80 nm in height with an area density of $69/\mu\text{m}^2$. The size of cranberries slightly increased to $106 \pm 26 \text{ nm}$ in diameter and 100 nm in height (Figure 3c) after grafting the first generation PEI (MW = 10 000 g/mol). Interestingly, seed-like nanomotifs, $16.4 \pm 3.8 \text{ nm}$ in diameter, started to appear between the nano-cranberry domes. According to the radius of gyration (R_g) of branched PEI (MW = 10 000 g/mol), 3.95 nm ,³⁵ each “nanoseed” should consist of at least ~ 4 PEI chains tethered to the SU-8 surface assuming that they do not overlap, although the opposite case is more likely. They appear hemispherical in shape to minimize unfavorable interactions between the relatively hydrophilic PEI chains and relatively hydrophobic SU-8 surface. When two more alternating layers of SR399 and PEI were grafted, the cranberries began to look like strawberries with “nano-seeds” visible on top of and between the nanodomains (Figure 3d). The overall diameter and height of the “nano-strawberries” were close to those of the cranberries, $112 \pm 24 \text{ nm}$ in diameter and 98

nm in height, and the size of “nano-strawberry” seeds increased to $18.6 \pm 5.3 \text{ nm}$ in diameter. After the sixth generation, the “nano-strawberries” transformed into surface with a texture that appear like “nano-raspberries” (Figure 3e), $109 \pm 22 \text{ nm}$ in diameter and 99 nm in height. The “nano-raspberry” seeds are larger than the “nano-strawberry” seeds, $20.6 \pm 5.4 \text{ nm}$, indicating further growth of the hyperbranched brushes on surface. When ten generations of PEI were grafted to the surface, the nanodomains began to resemble pineapples (Figure 3f), $111 \pm 27 \text{ nm}$ in diameter and 80 nm in height, whereas the “nanoseeds” seemed to appear smoothing out. This smoothing phenomenon could be explained by the space filling effect as the HPEA chains continue to grow in complexity and length. The polymer chain ends extend further away from the SU-8 surface, therefore masking the nanodomains. Meanwhile, the branching of the polymer grafts causes crowding between brushes. Because both SR399 and PEI chains have multiple sites for Michael addition, interchain and intrachain cross-linking within and between the layers becomes possible and is favored because of steric hindrance.

The surface morphology, however, was completely different when the SU-8 surface was initially treated with APTES in toluene. Phase AFM images show that the APTES-treated SU-8 surface is rather smooth and uniformly covered with nanomotifs ($19.4 \pm 5.6 \text{ nm}$) (Figure 4a). No further change of surface coverage was observed after PEI

(35) Park, I. H.; Choi, E. J. *Polymer* **1996**, *37*, 313.

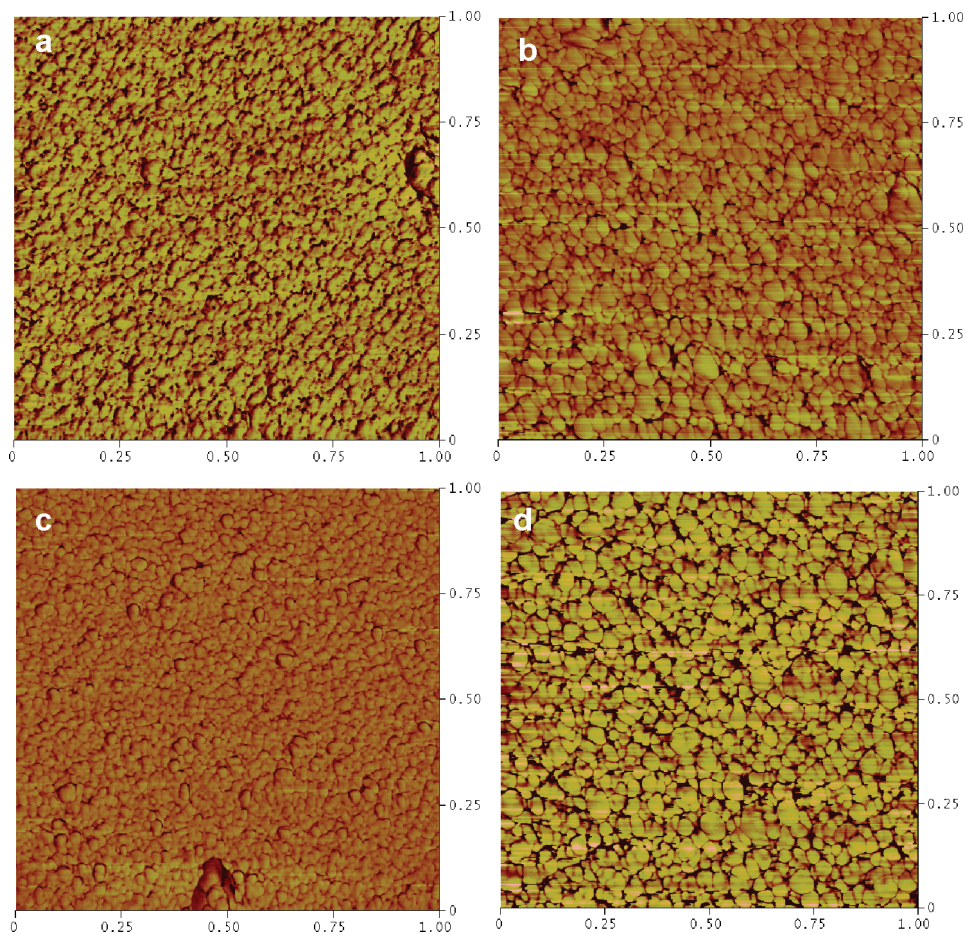


Figure 4. Phase AFM images of SU-8 films treated with APTES/toluene solution (a), followed by grafting of PEI (MW = 10 000 g/mol): (b) G1, (c) G3, and (d) G6. Scale = $1 \mu\text{m} \times 1 \mu\text{m}$.

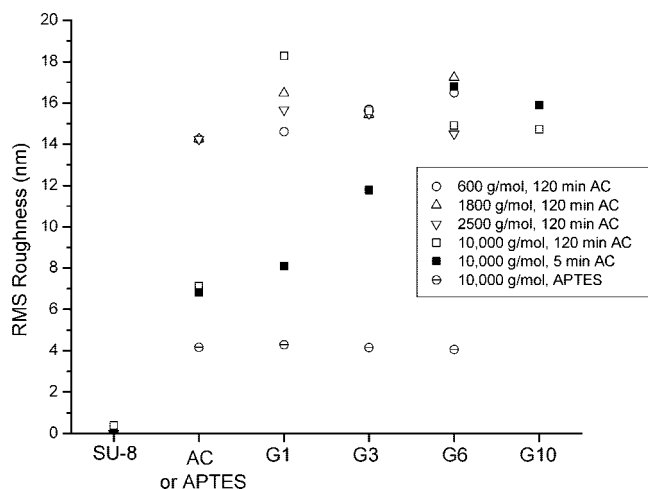


Figure 5. Surface rms roughness versus generation of HPEA from different molecular weight PEIs grafted on photo-crosslinked SU-8, which was treated with 100 mM acryloyl chloride (AC)/toluene for 5 or 120 min, or APTES/toluene for 120 min.

grafting (Figure 4b–d). The size of the nanomotifs increased to 34.1 ± 11.2 nm (G1), and remained more or less constant at higher generations, 27.6 ± 11.3 (G3) and 39.0 ± 11.4 nm (G6), respectively. The apparent morphology difference between the AC and APTES treated surfaces is further supported by the rms roughness analysis (Figure 5). For the latter, the rms roughness remains ~ 4 nm for all samples, regardless of the generation. In contrast, the rms roughness

of the AC modified surfaces varies depending on treatment time and generation. The SU-8 surfaces increase in rms roughness from 0.4 nm to 7–14 nm after treatment with AC, and to ~ 17 nm at generation 6. This indicates that the overall surface roughness is dominated by the nanodomains.

The immediate question is what causes the initial formation of the “nano-cranberry” domes. Since toluene was the solvent in both AC and APTES treatment of SU-8 and no nanodomains were observed when soaking the crosslinked SU-8 in toluene by itself, it was first thought that reaction between AC and the surface hydroxyl groups was responsible for dome formation. However, SU-8 surfaces were nearly featureless when exposed to neat AC or to AC dissolved in methylene chloride, acetone, tetrahydrofuran, and acetonitrile, where the films tended to delaminate from a glass substrate. Very sparsely distributed dome-like features were observed when the SU-8 film was exposed to AC solutions in ethyl acetate and dioxane. When SU-8 was treated with AC solutions in toluene, anisole, and xylene, a high density of nanodomains popped up on the surface, with dome size slightly increased in the order of anisole < toluene < xylene (Figure 6). This observation suggests that both solvent quality and reaction between AC and SU-8 surface play an important role in the formation of nanodomains.

To verify the hypothesis, we estimated the polymer–solvent interactions by calculating relative energy difference (RED) numbers and Flory–Huggins interaction parameters, χ , using

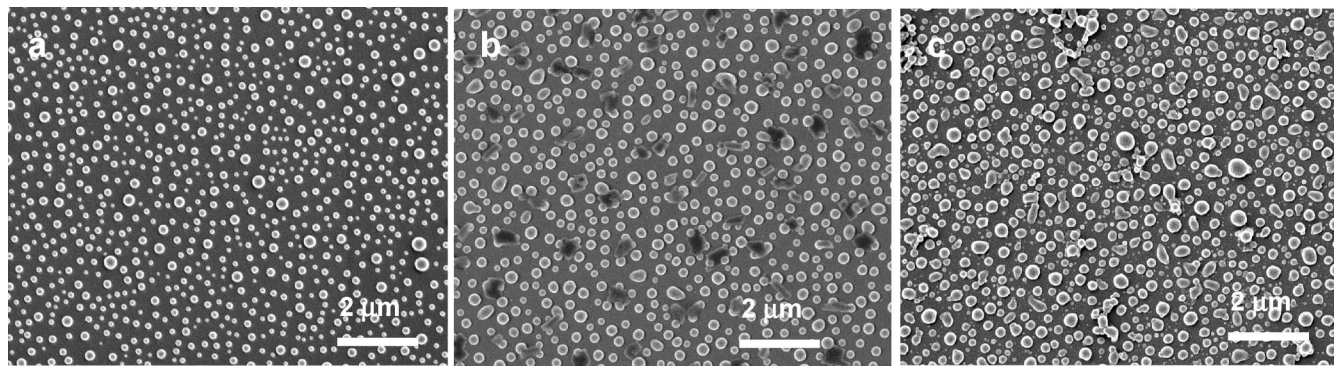


Figure 6. SEM images of SU-8 films treated with 100 mM acryloyl chloride in different solvents for 120 min: (a) anisole, (b) toluene, (c) xylene.

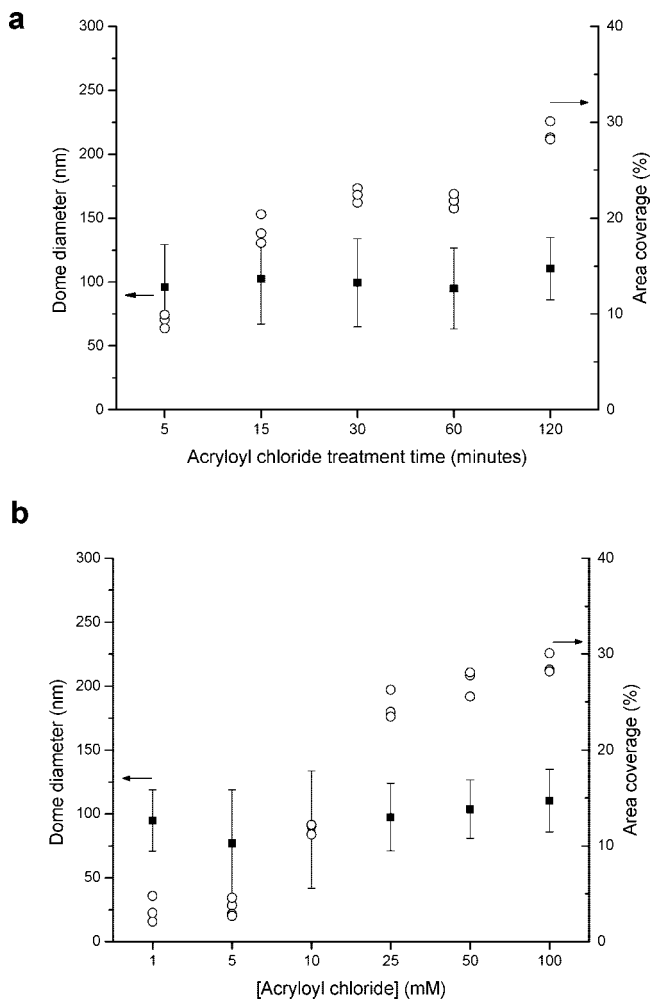


Figure 7. Size and surface area coverage percentage of the “nano-cranberry” domes formed on SU-8 surfaces treated with (a) 100 mM acryloyl chloride/toluene solutions for various times, and (b) various acryloyl chloride/toluene concentrations for 120 min.

Hansen solubility parameters³⁶ (see the Supporting Information). Because the solubility parameter of SU-8 is not available, we used the value of Epon 1001 (Shell Chemical Corp.), a similar bisphenol A epoxy resin, as an approximation. $RED < 1.0$ and $\chi < 0.5$ indicates a high affinity between the polymer and the solvent, $RED > 1.0$ and $\chi > 0.5$ indicates poor solubility of the polymer in a given solvent,

and $RED = 1.0$ and $\chi = 0.5$ indicates a boundary condition where the polymer partially dissolves in a given solvent. As seen in Table S1, although the order of polymer–solvent affinity predicted by RED and χ values may not match exactly, which may be attributed to the approximation of the Epon 1001 to SU-8, their analysis vs the experimental observation clearly implies that domes are formed when acryloyl chloride, a very good solvent of SU-8 ($RED = 0.58$, $\chi = 0.22$), is dissolved in a relatively poor solvent of SU-8, such as toluene. While toluene softens the crosslinked SU-8 surface, AC could preferentially swell and penetrate into the network and react with hydroxyl groups, leading to the nanodome formation. Upon solvent evaporation, the domes are locked in the glassy SU-8 matrix. Therefore, the dome size and density should be a function of the crosslinking density, hydroxyl group surface coverage, and swellability of the SU-8 film. Supporting this, we found that the size of the domes did not change with treatment time or concentration of AC. However, the surface coverage of the domes varies with AC/toluene treatment time and concentration (Figure 7). For example, the area density of nanodomains increased from to $19/\mu\text{m}^2$ to $69/\mu\text{m}^2$ (Figure 3b), corresponding to 5 and 120 min treatments, respectively. When APTES is used to treat the SU-8 surfaces, the reactions can occur between the alkoxy groups in APTES and multiple hydroxyl groups on the SU-8 surface or by the autocondensation of APTES itself. We suspect that a glassy, multilayered polysiloxane network, $(-\text{O}-\text{Si}-\text{O})_x$, might conformally coat the SU-8 surface, thus, preventing solvent from diffusion into the inner SU-8 network to form any dome. In a similar vein, we could explain the results by the difference in polarity between AC, APTES, SU-8 surface, and toluene. The presence of a relatively nonpolar vinyl group in AC improves the interaction between the nonpolar SU-8 surface (water contact angle $\sim 80^\circ$) and the aromatic solvent, whereas very polar amino and alkoxy groups in APTES do not interact with toluene and SU-8 effectively.

To complete the study, we grafted PEIs with different molecular weights and architectures to investigate their influence to the size and density of “nano-fruits” grown on SU-8 surfaces. PEI of 600, 1800, and 10 000 g/mol have a branched backbone, whereas 2500 g/mol PEI is linear. Branched PEI contains primary, secondary, and tertiary amines in a ratio of 1:2:1, whereas linear PEI contains only secondary amines in the backbone and primary amine-

(36) Hansen, C. M., *Hansen Solubility Parameters: A User's Handbook*; CRC Press: Boca Raton, FL, 2000.

terminated chain ends. Secondary amines have been shown to be more reactive than primary amines in the formation of hyperbranched PAMAM polymers.³⁷ In our system, however, primary amines can react with two acrylate groups, leading to the formation of an additional branch point.

As seen in Figure S1 in the Supporting Information, similar nanodome morphologies (Figure 3c) were observed in all cases after the SU-8 surface was treated with AC in toluene, followed by grafting of G1 PEI (see a, c, and e in Figure S1 in the Supporting Information), except that the nanoseeds between the cranberries were much smaller, 12.1 ± 3.1 , 11.3 ± 3.1 , and 12.9 ± 4.1 nm in diameter for 600, 1800, and 2500 g/mol, respectively, in comparison to 16.4 ± 3.8 nm for 10,000 g/mol. This result further confirms that the initial nanodome formation should be attributed to the synergistic interactions between acryloyl chloride, toluene and SU-8. After six generations of grafting (see b, d, and f in Figure S1 in the Supporting Information), nanoseeds were visible both on top of and between the nanodomains, and nearly completely covered the SU-8 surface. Within experimental errors, the seed size did not vary much up to G6, 11.0 ± 2.5 , 10.4 ± 2.4 , and 13.6 ± 3.8 nm for the 600, 1800, and 2500 g/mol PEI, respectively. These results differ from the 10 000 g/mol PEI case, which can be attributed to the smaller R_g of these polymers, 1.18, 1.89, and 0.82 nm for 600, 1800, and 2500 g/mol PEI, respectively, compared to 3.95 nm for 10 000 g/mol PEI.^{35,38} Because of the hyperbranched nature and size scale of these layer-by-layer grafted polyamines, stringent conclusions regarding the influence of the initial PEI architecture versus the seed size and density could not be drawn.

Conclusions

We have explored a new surface amplification strategy by grafting hyperbranched poly(ester amine) (HPEA) brushes on patterned SU-8 templates through alternating layer-by-

layer Michael reactions between PEI and SR399. By varying the initial surface functionalization chemistry and solvent, we observed the development of hierarchical nanofruits with a high density of functional groups (amine and acrylates) on SU-8 surfaces over generations. During the initial surface acrylation in toluene, nanodomains (on the order of 100 nm in diameter) were formed, because of the heterogeneous swelling of a crosslinked SU-8 network by aromatic solvents and acryloyl chloride molecules. The subsequent grafting of HPEA led to the appearance of seedlike nanostructures (on the order of 10 nm) between and on top of the nanodomains, forming various nanofruits on SU-8 surfaces. We can control the morphology and complexity of the nanofruits by varying the initial acrylation time, concentration, solvent, and the molecular weight of PEI, as well as the generation of the hyperbranched polymer grafts. This process takes place on a photopatterned substrate, enabling us to harness the potential of hierarchical architectures and nanomaterials for various applications, including surface wetting, adhesion, and biomimetic mineralization. We have recently attempted silica deposition on HPEA nanofruits grown on SU-8 micropillars that show interesting wetting behaviors, allowing us to elucidate the necessity of dual roughness for superhydrophobic surfaces.

Acknowledgment. We thank Dr. Guojie Wang for initiating the layer-by-layer grafting strategy. This research is supported by the Office of Naval Research (ONR), Grant N00014-05-0303, and National Science Foundation (NSF) CAREER award, DMR-0548070.

Supporting Information Available: (1) Phase AFM images of nanofruits generated from PEI with molecular weights of 600, 1800, and 2500 g/mol, and (2) Hansen solubility parameters and relative energy difference (RED) numbers of various polymer/solvent systems (PDF). This material is available free of charge via the Internet at <http://pubs.acs.org>.

CM801913Q

(37) Wang, D.; Zheng, Z.; Hong, C.; Liu, Y.; Pan, C. *J. Polym. Sci., Part A* **2006**, *44*, 6226.

(38) Sasanuma, Y.; Hattori, S.; Imazu, S.; Ikeda, S.; Kaizuka, T.; Iijima, T.; Sawanobori, M.; Azam, M. A.; Law, R. V.; Steinke, J. H. G. *Macromolecules* **2004**, *37*, 9169.